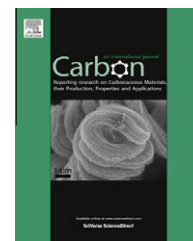


Available at www.sciencedirect.com

SciVerse ScienceDirect

journal homepage: www.elsevier.com/locate/carbon

The reason for the low density of horizontally aligned ultralong carbon nanotube arrays

Rufan Zhang ^a, Huanhuan Xie ^{a,b}, Yingying Zhang ^{b,*}, Qiang Zhang ^a, Yuguang Jin ^a, Peng Li ^{a,b}, Weizhong Qian ^a, Fei Wei ^{a,b,*}

^a Beijing Key Laboratory of Green Chemical Reaction Engineering and Technology, Tsinghua University, Beijing 100084, China

^b Center for Nano and Micro Mechanics, Tsinghua University, Beijing 100084, China

ARTICLE INFO

Article history:

Received 10 May 2012

Accepted 15 September 2012

Available online 24 September 2012

ABSTRACT

The reason why few carbon nanotubes (CNTs) nucleated in the catalyst region on substrates grow into ultralong ones during gas flow directed chemical vapor deposition (CVD) of horizontally aligned CNT arrays was explored. Small catalyst nanoparticles tend to merge into large ones due to the high processing temperature, which accordingly produces multi-wall CNTs (MWCNTs). These MWCNTs usually follow a base-growth mechanism and cannot be guided by the gas flow during growth. These MWCNTs are often shorter than 20 μm . Only the CNTs that follow the tip-growth mechanism, which are catalyzed by smaller nanoparticles and have fewer walls than most of the CNTs, tend to grow into longer ones. Besides, other factors influencing the areal density of ultralong CNTs, such as the entanglement of CNTs and the falling down of the growing tip of floating CNTs to the substrate, were also discussed.

© 2012 Elsevier Ltd. All rights reserved.

1. Introduction

Ultralong carbon nanotubes (CNTs) usually refer to the horizontally aligned CNT arrays with length up to centimeters or even decimeters grown on flat substrates by chemical vapor deposition (CVD) methods [1–4]. Due to their perfect structures and extraordinary thermal, electrical and mechanical properties, they show great potential as building blocks for nano-electronics [5], superstrong fibers [2,6], and even space elevators [7]. For the practical application of ultralong CNTs, the key is to realize the bulk production of ultralong CNTs with controlled structures. However, the main obstacle for the bulk production of ultralong CNTs is their extremely low areal density. The areal density of ultralong CNTs is usually several CNTs per 100 μm [3–5,8–10], which is far lower than that of agglomerated CNTs [11] and vertically aligned CNT arrays.

Arc-discharge, laser ablation, and CVD are the main methods for CNT synthesis. Compared with the other two

methods, CVD has many advantages in controlling the growth of CNTs, especially ultralong CNTs. It has a number of controllable variables, such as temperature [12], feeding gases [13], and catalysts [14], enabling the easy control of the growth process [15]. Both metal and nonmetal nanoparticles were used to catalyze the growth of CNTs [16]. Fe, Cu, Co, Mo, and Ni nanoparticles are the most widely used metal catalysts for producing ultralong CNTs using CVD methods [3,14,17]. The diameter of CNTs are proportionally related to the size of the catalytic nanoparticles [18,19]. Controlling the structure of catalytic nanoparticles allows the variation of diameter, length and even the chirality of CNTs [19].

A “kite mechanism” has been proposed for the growth of ultralong CNTs [20]. During a CNT growing process, one end of the CNT is floating over the substrate because of the thermal buoyancy caused by the temperature difference between the substrate and the flow gas. The catalyst nanoparticle is at the floating end of the CNT, which follows a tip-growth

* Corresponding authors.

E-mail addresses: yingyingzhang@tsinghua.edu.cn (Y. Zhang), wf-dce@tsinghua.edu.cn (F. Wei).

0008-6223/\$ - see front matter © 2012 Elsevier Ltd. All rights reserved.

<http://dx.doi.org/10.1016/j.carbon.2012.09.025>

mechanism (Fig. 1a). The kite-mechanism successfully explained many facts, such as ultralong CNTs could continuously grow up to 20 cm long [3] and cross over obstacles and trenches on substrates [5,20]. For short CNTs, they were considered to follow a base-growth mechanism [17], in which the catalyst nanoparticles anchored on substrate during CNTs growth (Fig. 1b). To date, many progresses have been made on synthesizing ultralong CNTs and continuous research is ongoing [16]. However, it is still a challenge to improve the areal density of ultralong CNTs. In this work, the reason for few CNTs obtained in the catalyst region on substrates can grow into ultralong ones during gas flow directed CVD growth was explored.

2. Experimental

2.1. CNT growth

The growth of CNTs was carried out in a tube furnace equipped with a quartz tube (Length: 1.5 m, outer/inner diameter: 35 mm/31 mm). Single crystal silicon wafers (3–10 cm long, 0.5–1 cm wide and 0.5 mm thick) with a 500-nm-thick SiO₂ layer on the surface were employed as substrates. An ethanol solution of FeCl₃ (0.03 mol L⁻¹) was coated onto the upstream end of the substrates. After reduction in H₂ and Ar (H₂:Ar = 2:1 in volume with a total flow of 200 sccm) at 900 °C for 25 min, the precursor FeCl₃ became Fe nanoparticles which worked as the catalysts for CNT growth. Then, the sample was heated from 900 to 1000 °C in two minutes and the inlet gas was switched to CH₄ and H₂ (CH₄:H₂ = 1:2 in volume with a total flow of 75 sccm), together with 0.43% H₂O for accelerating the CNT growth. The growth duration for the CNTs was usually 10–20 min, which depended on the length of CNTs desired.

2.2. Characterization

The CNTs were characterized by a scanning electron microscope (SEM, JSM 7401F, 1.0 kV), a high-resolution transmission electron microscope (HRTEM, JEM-2010, 120.0 kV) and an atomic force microscope (AFM, Veeco Nanoscope).

3. Results and discussion

3.1. The comparison of ultralong and short CNTs

The inset of Fig. 2 shows the morphology of CNTs grown on the substrate surface, where two regions can be observed. The left side is the catalyst region (shown by a yellow rectangle), consisting of a high density of randomly oriented short CNTs. The right side is the ultralong CNT region. Most of the as-grown ultralong CNTs are straight and parallel to the gas flow direction. The length of ultralong CNTs ranges from several millimeters to several centimeters. They are well separated with each other. The number distribution of ultralong CNTs along their axial direction is shown in Fig. 2. With increasing distance from the catalyst region, the number of ultralong CNTs only showed a moderate decrease. It seems that the maximum length of the ultralong CNTs grown by this method is mainly limited by the length of the substrates and the length of the high temperature zone of the furnace.

The areal density of the ultralong CNTs is far lower than that of short CNTs at the catalyst regions (Fig. 3). In the catalyst regions, there are numerous short CNTs which are randomly oriented on the substrates (Fig. 3b and c). However, only a few of them grow out of the catalyst regions and form ultralong CNTs, which were guided by the gas flow and parallel with each other.

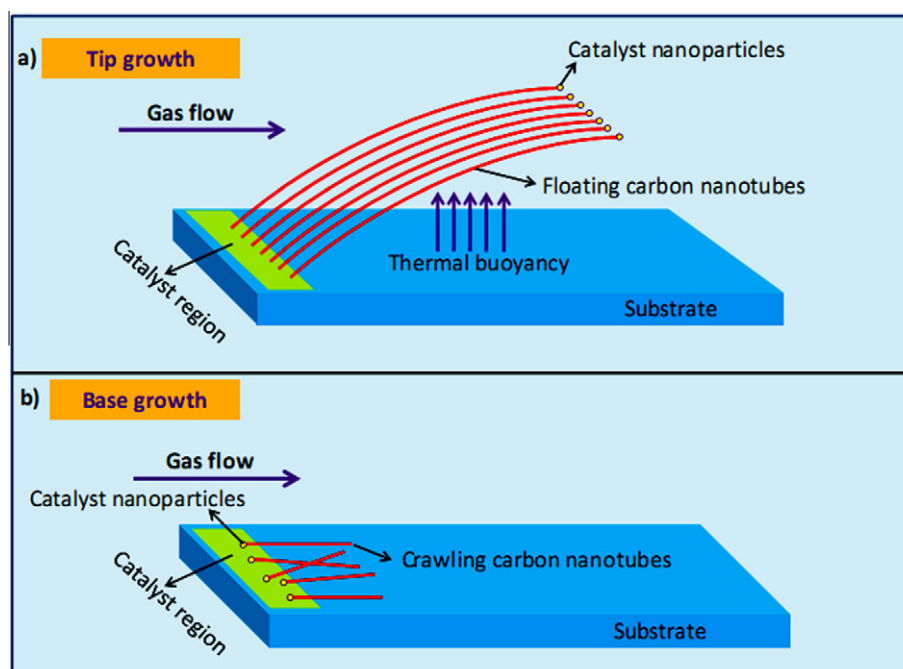


Fig. 1 – The scheme of tip-growth mechanism (a) and base growth mechanism (b) for CNTs.

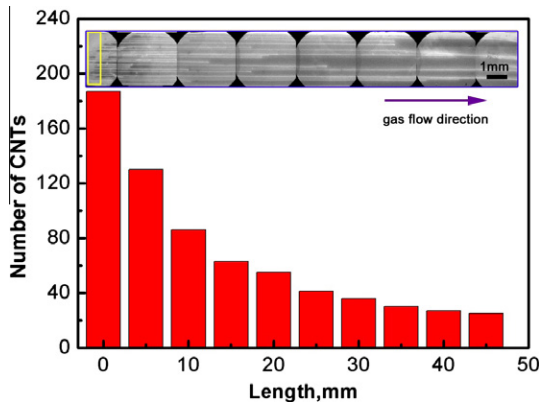


Fig. 2 – The number distribution of ultralong CNTs along their axial direction. The inset is a series of SEM images of ultralong CNTs taken along their axial direction. The yellow rectangle refers to the catalyst region. (For interpretation of the references to color in this figure legend, the reader is referred to the web version of this article.)

The length of short CNTs distributed in the catalyst regions is typically less than 20 μm . These short CNTs normally have one end embedded within catalyst islands (Fig. 3d). They were overlapped and entangled with each other. As shown in Fig. 3c and d, many of the starting ends of the tussocky short CNTs were from big catalyst islands (shown by the blue curves in Fig. 3c and d), which can be regarded as their “root”.

Besides, no catalyst nanoparticles can be seen at the free ends of these tussocky short nanotubes, while large number of nanoparticles can be found at the “root” ends of them. Therefore the randomly oriented short CNTs mostly follow the base-growth mechanism. In contrast, the ultralong CNTs are parallel to the gas flow direction. From the inset of Fig. 3b, we can clearly see there is a catalyst nanoparticle at the free end of an ultralong CNT. The ultralong CNTs were believed to float over the substrate and guided by the gas flow during growth as illustrated by the kite mechanism. Only those occasionally lifted CNTs by thermal buoyancy with Fe nanoparticles at the floating ends have the chance to growth into ultralong ones (Fig. 3b). Their growth were assumed to follow the tip growth mechanism [20].

3.2. The mechanism for short CNTs exhibiting limited length and random orientation

According to the base-growth mechanism, the catalysts stay on the substrate throughout the whole growth process, the strong van der Waals interaction between the CNTs and the substrate surface causes the termination of the growth when the CNTs reach certain length (such as 10 μm). The interaction between the CNTs and the SiO_2/Si surface is about 10 pN/nm [21]. In the base-growth mechanism of a CNT, since the whole CNT needs to slide on the substrate, the nanotube/substrate interaction would increase as a function of the length. The growth eventually stops when the force needed

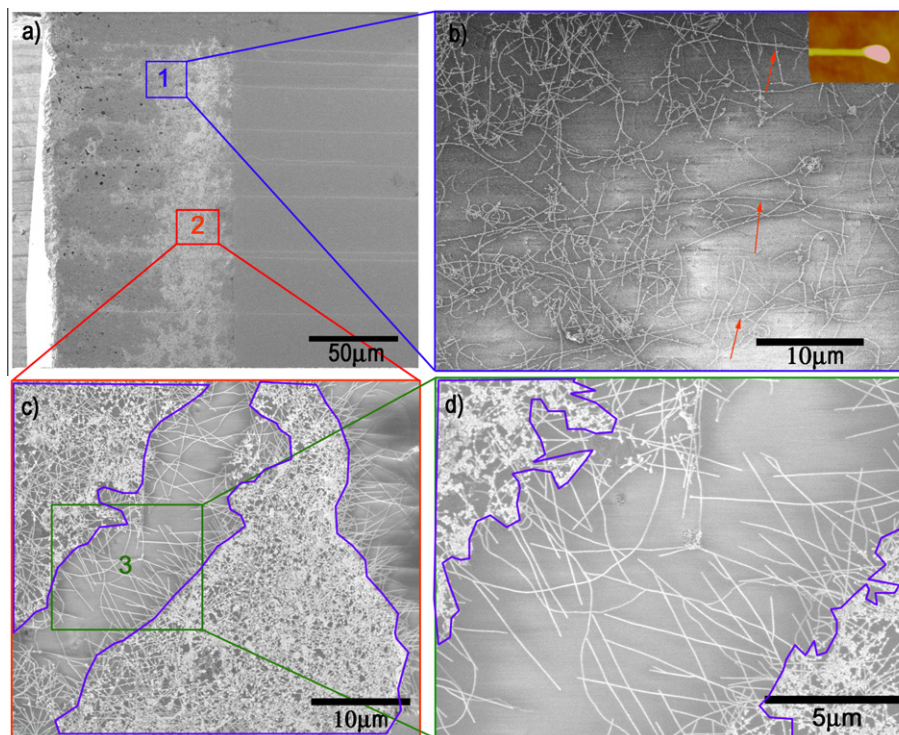


Fig. 3 – (a) The morphology of CNTs in catalyst region on substrates. (b) The enlargement of the selected area 1 in (a), where three ultralong CNTs (shown by the red arrows) lie across randomly oriented short CNTs. Inset: AFM image of an ultralong CNT with a catalyst nanoparticle on its tip end. (c) and (d) The enlargement of the selected area 2 in (a), showing tussocky short CNTs. The areas in blue curves are the catalyst islands. (For interpretation of the references to color in this figure legend, the reader is referred to the web version of this article.)

to move the whole CNT becomes energetically unfavorable, leading to the deactivation of the catalyst and the formation of a short CNT. Besides, the interaction between the densely tangled and overlapped short CNTs also hindered their growth [22].

The flow of a fluid can be divided into the laminar flow and the turbulent flow according to Reynolds number Re [23]. $Re = \rho v d / \mu$, where ρ is the gas density, v is the gas velocity, d is the diameter of the quartz tube and μ is the viscosity of the gas. When $Re < 2000$, the flow belongs to the laminar flow; otherwise, it belongs to the turbulent flow. Here, under our experimental conditions, Re is 0.081, which is far lower than 1, so the gas flow is a laminar flow (see [Supplementary information](#) for calculation details). For the laminar flow, the velocity profile in a cylinder tube is a parabola (Fig. 4a) according to the fluid mechanics theory.

The velocity distribution along the radial direction of the quartz tube can be expressed as $u = u_{\max}(1 - \frac{r^2}{R^2})$, where u is the velocity at the radial distance r from the axis of the quartz tube, u_{\max} is the highest velocity at the axis of the quartz tube and R is the radius of the quartz tube (15.5 mm for our case) (see Fig. 4b). According to the above equation, the velocity of gas flow around short CNTs (<20 μm) is nearly zero and almost stagnant, which has almost no dragging effect on CNTs within this layer (see [Supplementary information](#) for calculation details).

On the other hand, we can also get some ideas from the comparison of different forces acting on the CNTs by a back-of-the-envelope calculation to know why the short CNTs have random orientations. There are four main forces acting on floating CNTs: gravity, dragging from gas flow, thermal buoyancy and a Hooke force arising from the rigidity of CNTs (see Fig. 4c) [24]. While for CNTs contacted with the sub-

strate, the van der Waals interaction between CNTs and the substrate should also be taken into consideration. Both the gravity and the thermal buoyancy per unit length are constant for a given CNT. The rigidity of CNTs is sufficient to oppose the gravity only at short length scales (0.8 μm) to keep a CNT from contacting the surface. For ultralong CNTs floating in the gas flow, the gravity and the thermal buoyancy should be equivalent with each other to keep the CNTs floating (the van der Waals interaction between the CNTs and the substrate can be negligible for the floating CNTs because it works only on a very small portion of CNTs that near to the substrate (on the order of nanometers) [25]). For CNTs vertical to substrate with length shorter than 0.8 μm , the dragging force is too small to make the rigid CNTs to bend with the gas flow. For CNTs not vertical to the substrate and shorter than 10 μm , they are easy to be attracted to the substrate due to the strong van der Waals interaction. Only for the CNTs longer than 20 μm and only partly contacted with the substrate (contact length shorter than several nanometers) the dragging force can overcome the van der Waals interaction and the CNTs be guided by the gas flow (see [Supplementary information](#) for calculation of dragging force).

3.3. The reason for the low density of ultralong CNTs

3.3.1. Influence of aggregation of catalyst nanoparticles

The ultralong CNTs tend to have fewer walls than the short CNTs. Fig. 5 shows that some CNTs are obviously thinner than others. In order to investigate their structures, the CNTs were characterized by HRTEM. Fig. 6 shows the HRTEM images of CNTs obtained from both the catalyst region and the ultralong CNT region. The ultralong CNTs are few-wall CNTs (FWCNTs), such as single-wall CNTs (SWCNTs),

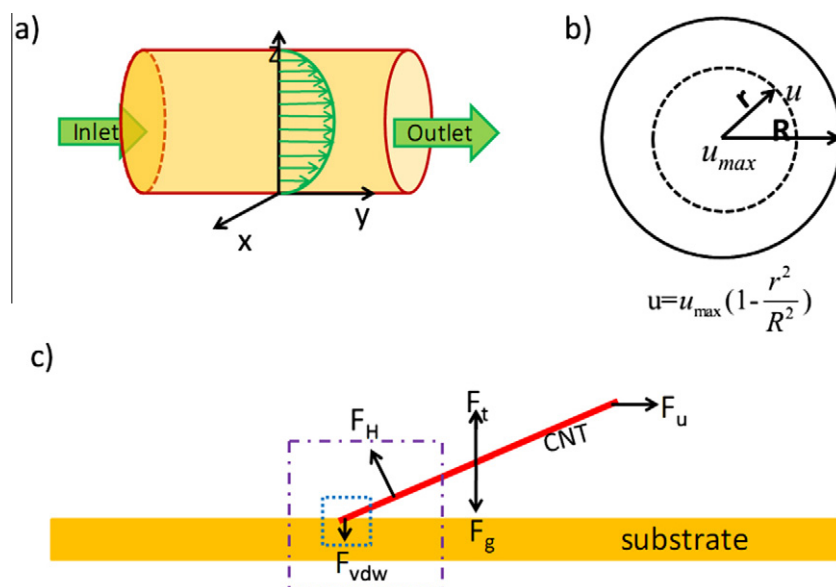


Fig. 4 – (a) and (b) The scheme of gas velocity distribution for laminar flow in a quartz tube. **(c)** The forces exerted on CNTs. F_u is the dragging force from gas flow. F_t is the thermal buoyancy from temperature difference. F_g is gravity. F_H is Hooke force from rigidity of CNTs. F_{vdw} is the van der Waals interaction between CNTs and the substrate. The purple square (large square) shows the working scale for F_H , and the blue square (small square) shows the working scale for F_{vdw} . (For interpretation of the references to colour in this figure legend, the reader is referred to the web version of this article.)

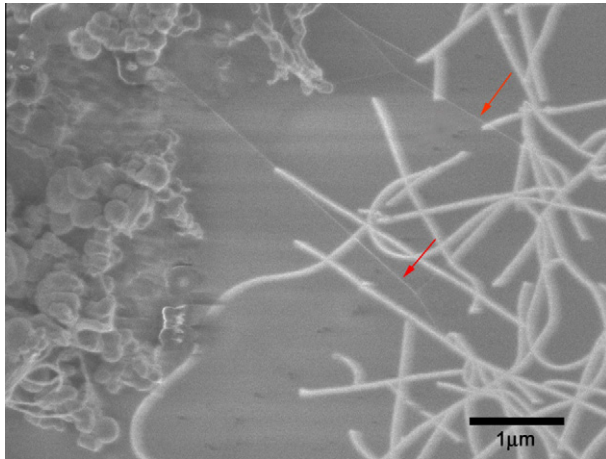


Fig. 5 – SEM image of CNTs in catalyst region. The red arrows show two CNTs with smaller diameters. The other thick curved structures in white are CNTs with large diameters. (For interpretation of the references to color in this figure legend, the reader is referred to the web version of this article.)

double-wall CNTs (DWCNTs) and triple-wall CNTs (TWCNTs). These FWCNTs have perfect structures and small diameters of ca. 1–4 nm, as shown in Fig. 6a–c. However, almost all of the short CNTs are MWCNTs with many structural defects (Fig. 6c and d). There are also many anomalous structures. These MWCNTs and anomalous structures usually have diameter of tens to hundreds of nanometers.

The growth of MWCNTs is mainly caused by the aggregation of catalyst nanoparticles enabled by the high processing

temperature. Fig. 7a–c shows that there are many metal clusters with different sizes in catalyst region on the substrate. The number of walls and diameter of CNTs are mainly determined by the size of catalyst nanoparticles at the initial stage of growth [18,19]. At the high temperature (1000 °C) used for growth of CNTs, small catalyst nanoparticles in catalyst region tend to merge into large ones to reduce their surface energy, which accordingly promote the growth of MWCNTs. From Fig. 7d, we can see that the typical diameter of large catalyst clusters ranges from tens to hundreds of nanometers, which are consistent with that of MWCNTs, but far larger than that of FWCNTs. From Fig. 7e we can see that the diameter distribution of MWCNTs is similar with that of catalyst nanoparticles. These MWCNTs tend to follow base-growth mechanism due to the strong interactions between the large catalyst nanoparticles and the substrate, which does not benefit their growth into ultralong ones. Only those isolated small catalyst nanoparticles can catalyze the growth of FWCNTs with a tip-growth mechanism. Therefore, it is crucial to prevent the agglomeration of catalyst nanoparticles and to create an upward force to lift up more CNTs for producing a high density of ultralong CNTs.

3.3.2. Influence of entanglement of short CNTs

From Figs. 3, 5 and 7, we can see that there are many entanglements of short CNTs at the catalyst area. The entanglement could be an obstacles which hinders the CNTs from being lifted up to float in the gas flow. From Fig. 4c and the force analysis of CNTs we know that the probable reason for the entanglement and the random orientation of the short CNTs is their short length, which makes it difficult for them to be guided by gas flow. Thus it is crucial to reduce the

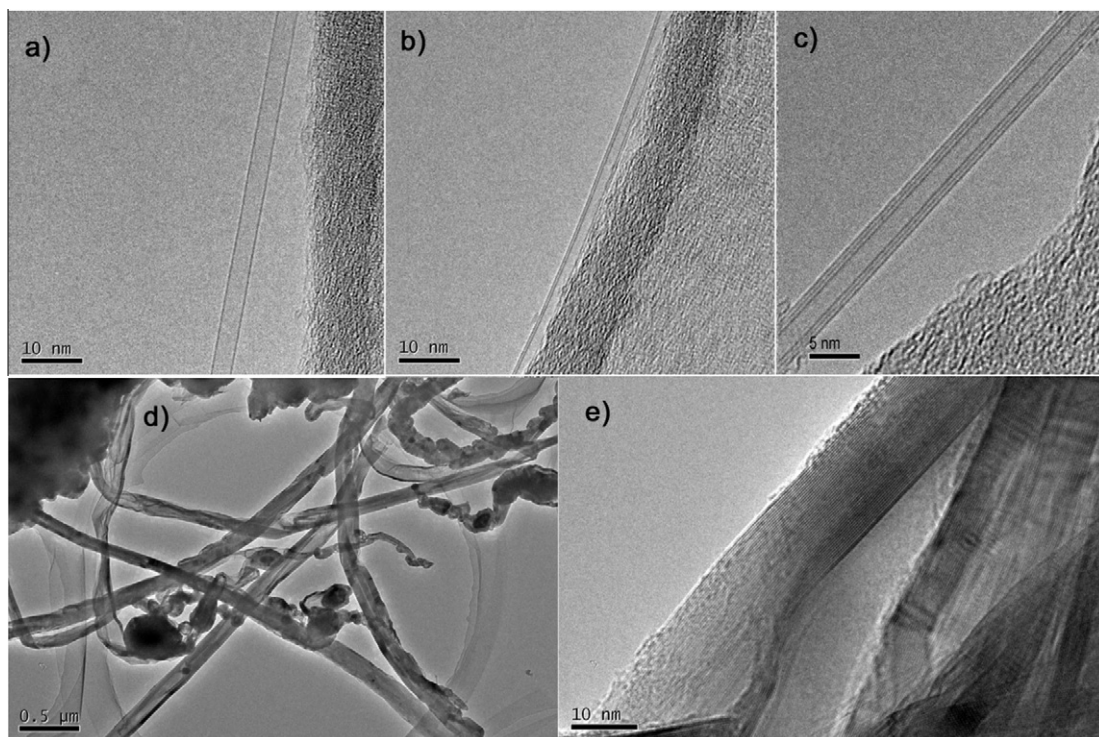


Fig. 6 – (a)–(c), TEM images of a SWCNT (a), a DWCNT (b) and a TWCNT (c) (d) and (e), TEM images of as-grown MWCNTs with structural defects.

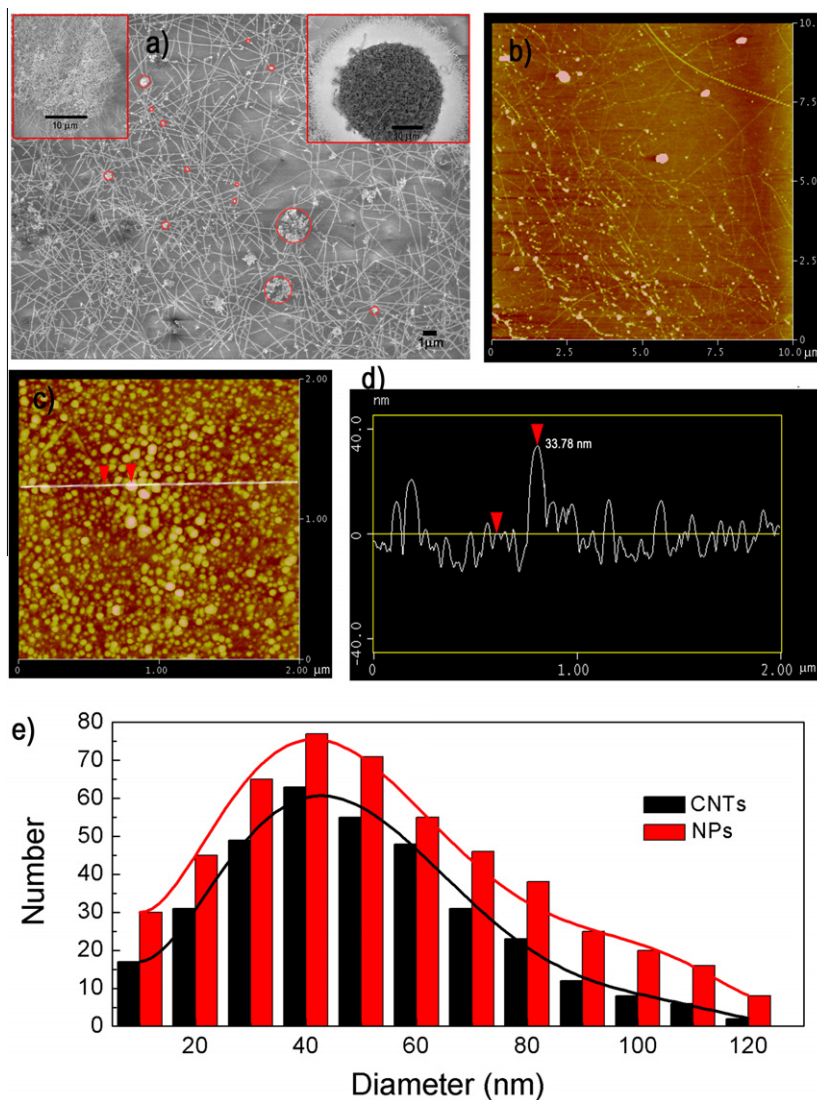


Fig. 7 – (a) SEM image of short CNTs and the catalyst nanoparticles in catalyst region. The red circles refer to catalyst particle clusters agglomerated from small metal nanoparticles at high temperature. The inset in the left corner is a typical region with a catalyst particle cluster. The inset in the right corner is a magnified image of a cluster. (b) AFM image of short CNTs in the catalyst region. (c) AFM image of agglomerated catalyst nanoparticles (d) Height profile of catalyst nanoparticles along the line shown in (c) (e) Diameter distribution of CNTs and catalyst nanoparticles (NPs). (For interpretation of the references to colour in this figure legend, the reader is referred to the web version of this article.)

catalyst aggregation to make more CNTs grow longer to decrease their entanglement and to obtain a higher areal density of them. Recently, by anchoring catalyst nanoparticles on silica nanospheres, we effectively reduced the catalyst aggregation and improved the areal density of ultralong CNTs (the result will be reported elsewhere).

3.3.3. Influence of falling down of growing tip of floating CNTs to the substrate

As shown in Fig. 2, many long CNTs gradually stopped growth and their density decreased, which may be induced by the falling down of the growing tips of floating long CNTs. There are probably several factors contributing to the falling down, such as CNT types, temperature variation, catalyst deactivation and gas flow disturbance, etc. For example, many reports have found that semiconducting CNTs are much easier than

metallic CNTs to grow into ultralong ones [3,4,8,13]. Adding of trace water during CNTs growth can effectively get rid of the amorphous carbon on the catalyst and improve the lifetime of catalysts, resulting in a much higher areal density of ultralong CNTs [3]. Stable gas flow was also found to be effective to improve the areal density of ultralong CNTs [5]. Therefore, to avoid the floating CNTs falling down to the substrate, a stable gas flow, improved catalyst lifetime, and stable temperature should be helpful.

4. Summary

We have investigated the difference between the structures of short CNTs and ultralong CNTs and interpreted their different growth mechanism. Due to the agglomeration of catalyst

nanoparticles on the substrate at high temperature, small nanoparticles tend to merge into large ones, which accordingly produced MWCNTs. These MWCNTs tend to follow base-growth mechanism due to the strong interaction between the large catalyst nanoparticles and the substrate, which hinders their extension into ultralong ones. Furthermore, these MWCNTs are usually shorter than 20 μm and are hard to be guided by gas flow due to the almost stagnant gas flow near the wall of the quartz tube and the weak dragging force acting on them, resulting in short and randomly oriented CNTs. The entanglement of CNTs is another obstacle blocking their growth. Only those FWCNTs with small diameters and with length longer than several hundred microns can be effectively directed by the gas flow. Besides, the falling down of growing tip of floating CNTs to the substrate is also one of the factors restricting the areal density of ultralong CNTs. In general, for effective growth of ultralong CNTs, the factors which should be taken into consideration include preventing the merging of small catalyst nanoparticles into large ones, creating an upward force to lift up more CNTs and providing a stable growing environment for ultralong CNTs.

Acknowledgement

This work is supported by the National Basic Research Program of China (2011CB932602) and the National Science Foundation of China (21203107).

Appendix A. Supplementary data

Supplementary data associated with this article can be found, in the online version, at <http://dx.doi.org/10.1016/j.carbon.2012.09.025>.

REFERENCES

- [1] Zheng LX, O'Connell MJ, Doorn SK, Liao XZ, Zhao YH, Akhadov EA, et al. Ultralong single-wall carbon nanotubes. *Nat Mater* 2004;3(10):673–6.
- [2] Zhang RF, Wen Q, Qian WZ, Su DS, Zhang Q, Wei F. Superstrong ultralong carbon nanotubes for mechanical energy storage. *Adv Mater* 2011;23(30):3387–91.
- [3] Wen Q, Zhang RF, Qian WZ, Wang YR, Tan PH, Nie JQ, et al. Growing 20 cm long DWNTs/TWNTs at a rapid growth rate of 80–90 $\mu\text{m/s}$. *Chem Mater* 2010;22(4):1294–6.
- [4] Wang XS, Li QQ, Xie J, Jin Z, Wang JY, Li Y, et al. Fabrication of ultralong and electrically uniform single-walled carbon nanotubes on clean substrates. *Nano Lett* 2009;9(9):3137–41.
- [5] Hong BH, Lee JY, Beetz T, Zhu YM, Kim P, Kim KS. Quasi-continuous growth of ultralong carbon nanotube arrays. *J Am Chem Soc* 2005;127(44):15336–7.
- [6] Zhang X, Jiang K, Feng C, Liu P, Zhang L, Kong J, et al. Spinning and processing continuous yarns from 4-inch wafer scale super-aligned carbon nanotube arrays. *Adv Mater* 2006;18(12):1505–10.
- [7] Edwards BC. Design and deployment of a space elevator. *Acta Astron* 2000;47(10):735–44.
- [8] Wen Q, Qian W, Nie J, Cao A, Ning G, Wang Y, et al. 100 mm long, semiconducting triple-walled carbon nanotubes. *Adv Mater* 2010;22(16):1867–71.
- [9] Liu Y, Hong JX, Zhang Y, Cui RL, Wang JY, Tan WC, et al. Flexible orientation control of ultralong single-walled carbon nanotubes by gas flow. *Nanotechnology* 2009;20(18):185601.
- [10] Ding L, Yuan D, Liu J. Growth of high-density parallel arrays of long single-walled carbon nanotubes on quartz substrates. *J Am Chem Soc* 2008;130(16):5428–9.
- [11] Wang Y, Wei F, Luo G, Yu H, Gu G. The large-scale production of carbon nanotubes in a nano-agglomerate fluidized-bed reactor. *Chem Phys Lett* 2002;364(5–6):568–72.
- [12] Yao Y, Li Q, Zhang J, Liu R, Jiao L, Zhu Y, et al. Temperature-mediated growth of single-walled carbon-nanotube intramolecular junctions. *Nat Mater* 2007;6(4):283–6.
- [13] Jin Z, Chu HB, Wang JY, Hong JX, Tan WC, Li Y. Ultralow feeding gas flow guiding growth of large-scale horizontally aligned single-walled carbon nanotube arrays. *Nano Lett* 2007;7(7):2073–9.
- [14] Li Y, Cui R, Ding L, Liu Y, Zhou W, Zhang Y, et al. How catalysts affect the growth of single-walled carbon nanotubes on substrates. *Adv Mater* 2010;22(13):1508–15.
- [15] Zhang Q, Huang JQ, Zhao MQ, Qian WZ, Wei F. Carbon nanotube mass production: principles and processes. *ChemSusChem* 2011;4(7):864–89.
- [16] Hong G, Chen Y, Li P, Zhang J. Controlling the growth of single-walled carbon nanotubes on surfaces using metal and non-metal catalysts. *Carbon* 2012;50(6):2067–82.
- [17] He M, Duan X, Wang X, Zhang J, Liu Z, Robinson C. Iron catalysts reactivation for efficient CVD growth of SWNT with base-growth mode on surface. *J Phys Chem B* 2004;108(34):12665–8.
- [18] Cheung CL, Kurtz A, Park H, Lieber CM. Diameter-controlled synthesis of carbon nanotubes. *J Phys Chem B* 2002;106(10):2429–33.
- [19] Li Y, Kim W, Zhang Y, Rolandi M, Wang D, Dai H. Growth of single-walled carbon nanotubes from discrete catalytic nanoparticles of various sizes. *J Phys Chem B* 2001;105(46):11424–31.
- [20] Huang SM, Woodson M, Smalley R, Liu J. Growth mechanism of oriented long single walled carbon nanotubes using “fast-heating” chemical vapor deposition process. *Nano Lett* 2004;4(6):1025–8.
- [21] Son H, Samsonidze GG, Kong J, Zhang Y, Duan X, Zhang J, et al. Strain and friction induced by van der Waals interaction in individual single walled carbon nanotubes. *Appl Phys Lett* 2007;90(25):253113.
- [22] Feng C, Yao Y, Zhang J, Liu Z. Nanobarrier-terminated growth of single-walled carbon nanotubes on quartz surfaces. *Nano Res* 2009;2(10):768–73.
- [23] Shaughnessy EJ, Katz IM, Schaffer JP. Introduction to Fluid Mechanics. New York: Oxford University Press; 2005.
- [24] Hofmann M, Nezich D, Reina A, Kong J. In-situ sample rotation as a tool to understand chemical vapor deposition growth of long aligned carbon nanotubes. *Nano Lett* 2008;8(12):4122–7.
- [25] Yao YG, Dai XC, Feng CQ, Zhang J, Liang XL, Ding L, et al. Crinkling ultralong carbon nanotubes into serpentines by a controlled landing process. *Adv Mater* 2009;21(41):4158–62.